Solution multiplicity and stick configurations in continuous and finite element friction problems

Patrick HILD *

Laboratoire de Mathématiques, Université de Franche-Comté / CNRS UMR 6623, 16 route de Gray, 25030 Besançon, France.

Abstract

This work is concerned with friction problems in linear elasticity. We consider the unilateral contact model with the static Coulomb friction law in the continuous and finite element contexts. Having at our disposal a solution of the problem where stick does not occur on the entire contact zone, we consider the simple problem which consists of checking if the stick configuration solves also the friction problem. We prove that this solution multiplicity phenomenon occurs in the continuous case when a solution with grazing contact exists. We perform the corresponding finite element computations as well as some ones dealing with separation solutions.

Keywords : stick configuration, Coulomb friction, unilateral contact, finite elements, linear elasticity, solution multiplicity.

1. Introduction

Finite element codes do not generally propose several solutions to the user when the problem under consideration admits more than a solution. On the one hand if the set of solutions is locally connected, one can easily imagine that convergence problems of the algorithms could occur. On the other hand if the set of solutions consists of several isolated points, the setting is quite different and a computed solution can be obtained with a good convergence of the algorithms although there exist other distant solutions.

This paper is concerned with the latter phenomenon in the case of the unilateral contact model with Coulomb friction in two and three space dimensions (see [4, 11]). In the simplest case of continuum static elasticity, this frictional contact problem shows important difficulties in its mathematical handling. The existence of a solution was proven in [12] in the case of a small friction coefficient (with generalizations concerning the geometries and improvements of the bound ensuring existence in [10, 5]). As far as we know there does not exist any nonexistence example for the continuous

*Tel.: (+33) 381666349; Fax: (+33) 381666623; E-mail: hild@math.univ-fcomte.fr

problem. On the one hand a first uniqueness result has been obtained very recently in [14] with the assumption that a regular solution exists and that the friction coefficient is sufficiently small. On the other hand there are at least three classes of explicit non-uniqueness examples in the continuous case:

- a first one involving an infinity of slipping solutions (none of them with stick anywhere on the contact zone) located on a connected set when the friction coefficient is a precise value (see [8]);
- a second class dealing with two isolated (here the denomination "isolated" means that the set of solutions is not connected) solutions (stick and strict separation) for large friction coefficients (see [9]);
- a third one which is exhibited in this paper and corresponding to two solutions (stick and grazing contact) for large friction coefficients.

An outline of the paper is as follows. In section 2 we consider a body lying on a rigid foundation in the continuum setting and we check if the stick configuration solves the friction problem when a first solution is known. We then prove in section 3 that the phenomenon exists (at least in some cases) when a first solution with grazing contact (zero density of surface forces and zero normal displacement on the contact zone) is known. We also recall the results obtained in [9] concerning solutions with strict separation from the foundation. In section 4 we carry out the finite element computations corresponding to the solution multiplicity phenomena considered in the previous sections.

2. The continuous problem and the stick criterion

Let be given a domain Ω in $\mathbb{R}^n, n = 2, 3$ which represents an elastic body in the initial unconstrained configuration. Its boundary $\partial\Omega = \overline{\Gamma}_D \cup \overline{\Gamma}_N \cup \overline{\Gamma}_C$ consists of three non-overlapping domains Γ_D, Γ_N and Γ_C where the measures (in $\mathbb{R}^{n-1}$) of Γ_D and Γ_C are positive. The body Ω is submitted to given displacements $\mathbf{U}$ on Γ_D, it is subjected to surface traction forces $\mathbf{F}$ on Γ_N and the body forces are denoted $\boldsymbol{f}$. In the initial configuration, the part Γ_C is considered as the candidate contact surface on a rigid foundation which means that the contact zone cannot enlarge during the deformation process. The contact is assumed to be frictional and the stick, slip and separation zones on Γ_C are not known in advance. The unit outward normal vector on $\partial\Omega$ is $\boldsymbol{n}$ and $\mu \geq 0$ stands for the friction coefficient on Γ_C.

The Coulomb friction problem in elastostatics with unilateral contact conditions is to find the displacement field $\boldsymbol{u} : \Omega \to \mathbb{R}^n, (n = 2, 3)$ satisfying (2.1)–(2.6):

$$\mathbf{div}\, \boldsymbol{\sigma}(\boldsymbol{u}) + \boldsymbol{f} = \mathbf{0} \quad \text{in } \Omega, \tag{2.1}$$

$$\boldsymbol{\sigma}(\boldsymbol{u}) = \mathbf{C}\, \boldsymbol{\varepsilon}(\boldsymbol{u}) \quad \text{in } \Omega, \tag{2.2}$$

where the notation $\boldsymbol{\sigma}(\boldsymbol{u})$ represents the stress tensor field lying in $\mathcal{S}_n$ the space of second order symmetric tensors on $\mathbb{R}^n$. The linearized strain tensor field is $\boldsymbol{\varepsilon}(\boldsymbol{u}) =$

$(\boldsymbol{\nabla u} + \boldsymbol{\nabla}^T \boldsymbol{u})/2$ and $\mathbf{C}$ is the fourth order symmetric and elliptic tensor of linear elasticity. Next we define the Dirichlet and Neumann conditions:

$$\boldsymbol{u} = \mathbf{U} \quad \text{on } \Gamma_D, \tag{2.3}$$

$$\boldsymbol{\sigma}(\boldsymbol{u})\boldsymbol{n} = \mathbf{F} \quad \text{on } \Gamma_N. \tag{2.4}$$

The following notation is adopted for any displacement field $\boldsymbol{u}$ and for any density of surface forces $\boldsymbol{\sigma}(\boldsymbol{u})\boldsymbol{n}$ defined on the boundary of Ω:

$$\boldsymbol{u} = u_n \boldsymbol{n} + \boldsymbol{u_t} \quad \text{and} \quad \boldsymbol{\sigma}(\boldsymbol{u})\boldsymbol{n} = \sigma_n(\boldsymbol{u})\boldsymbol{n} + \boldsymbol{\sigma_t}(\boldsymbol{u}),$$

where $\boldsymbol{u_t}\cdot\boldsymbol{n} = 0$ and $\boldsymbol{\sigma_t}(\boldsymbol{u})\cdot\boldsymbol{n} = 0$. On Γ_C, the three conditions representing unilateral contact are as follows:

$$\begin{cases} u_n \leq 0, \\ \sigma_n(\boldsymbol{u}) \leq 0, \\ \sigma_n(\boldsymbol{u})\, u_n = 0, \end{cases} \tag{2.5}$$

and the Coulomb friction law on Γ_C is summarized by the following conditions:

$$\begin{cases} \boldsymbol{u_t} = \mathbf{0} \implies |\boldsymbol{\sigma_t}(\boldsymbol{u})| \leq -\mu\sigma_n(\boldsymbol{u}), \\ \boldsymbol{u_t} \neq \mathbf{0} \implies \boldsymbol{\sigma_t}(\boldsymbol{u}) = \mu\sigma_n(\boldsymbol{u})\dfrac{\boldsymbol{u_t}}{|\boldsymbol{u_t}|}. \end{cases} \tag{2.6}$$

When $\mu = 0$ the friction law in (2.6) simply reduces to the condition $\boldsymbol{\sigma_t}(\boldsymbol{u}) = \mathbf{0}$ and the problem admits a unique solution [6]. Moreover it is easy to see that the solution $\boldsymbol{u} = \mathbf{0}$ is unique when $\mathbf{U} = \mathbf{F} = \boldsymbol{f} = \mathbf{0}$.

Remark 2.1 *We mention that the physically relevant Coulomb friction law involves the tangential contact velocities and not the tangential displacements. Nevertheless, a problem analogous to the one considered in (2.6) is obtained by time discretization of the quasi-static frictional contact evolution problem. In this case* $\boldsymbol{u}$*,* $\boldsymbol{f}$ *and* $\mathbf{F}$ *stand for* $\boldsymbol{u}((i+1)\Delta t)$*,* $\boldsymbol{f}((i+1)\Delta t)$ *and* $\mathbf{F}((i+1)\Delta t)$ *respectively and* $\boldsymbol{u_t}$ *has to be replaced by* $\boldsymbol{u_t}((i+1)\Delta t) - \boldsymbol{u_t}(i\Delta t)$*, where* Δt *denotes the time step. For simplicity and without any loss of generality only the static case described above will be considered in this work. Finally let us remark that from a mathematical point of view the same kind of result as for the static case (existence of a solution if the friction coefficient is small) has been obtained for the quasi-static problem in [2, 13].*

Now we consider a solution $\boldsymbol{u}$ of the unilateral contact problem with Coulomb friction (2.1)–(2.6) in which stick does not occur everywhere on the contact zone Γ_C. Having at our disposal this field verifying $\boldsymbol{u} \not\equiv \mathbf{0}$ on Γ_C, we check if the field with stick everywhere on the contact zone solves the contact problem. The problem is to find the displacement field $\bar{\boldsymbol{u}} : \Omega \to \mathbb{R}^n, (n = 2, 3)$ such that:

$$\begin{cases} \mathbf{div}\, \boldsymbol{\sigma}(\bar{\boldsymbol{u}}) = \boldsymbol{f} & \text{in } \Omega, \\ \boldsymbol{\sigma}(\bar{\boldsymbol{u}}) = \mathbf{C}\, \boldsymbol{\varepsilon}(\bar{\boldsymbol{u}}) & \text{in } \Omega, \\ \bar{\boldsymbol{u}} = \mathbf{U} & \text{on } \Gamma_D, \\ \boldsymbol{\sigma}(\bar{\boldsymbol{u}})\boldsymbol{n} = \mathbf{F} & \text{on } \Gamma_N, \\ \bar{\boldsymbol{u}} = \mathbf{0} & \text{on } \Gamma_C. \end{cases} \tag{2.7}$$

When the compatibility conditions at the possible common points of the boundary parts $\overline{\Gamma_D}$ and $\overline{\Gamma_C}$ are satisfied which we assume for the sake of simplicity (in fact this will be the case in all the forthcoming examples and numerical experiments), problem (2.7) admits a unique solution $\bar{\boldsymbol{u}}$. Let us mention that the fields we consider in this study are "regular". As a consequence, the normal and tangential stresses on the contact zone are at least defined almost everywhere.

The following proposition furnishes a sufficient condition for the non-uniqueness of the equilibrium solution $\boldsymbol{u}$ to problem (2.1)–(2.6).

Proposition 2.2 *Let $\boldsymbol{u}$ be a displacement field solving problem* (2.1)–(2.6) *such that $\boldsymbol{u} \not\equiv \mathbf{0}$ on Γ_C. Let $\bar{\boldsymbol{u}}$ be the solution of problem* (2.7)*. If $\mu > 0$ and $|\boldsymbol{\sigma_t}(\bar{\boldsymbol{u}})| \leq -\mu\sigma_n(\bar{\boldsymbol{u}})$ on Γ_C, then $\bar{\boldsymbol{u}}$ is another solution of Coulomb's frictional contact problem* (2.1)–(2.6).

Proof. Straightforward. □

3. Examples in the continuous context

We next show examples in two space dimensions where the solution $\boldsymbol{u}$ satisfies grazing contact or separates from the rigid foundation and which fulfill the assumptions of the Proposition 2.2.

3.1. *Case where u satisfies grazing contact*

We now search a field $\boldsymbol{u}$ solving (2.1)–(2.6) and verifying grazing contact (i.e., $u_n = \sigma_n(\boldsymbol{u}) = 0$ on Γ_C). If $\bar{\boldsymbol{u}}$ is a field satisfying the assumptions of the proposition, we denote

$$\boldsymbol{\varphi} = \bar{\boldsymbol{u}} - \boldsymbol{u}, \tag{3.1}$$

and we observe that $\boldsymbol{\varphi}$ is a nonzero displacement field satisfying:

$$\begin{cases} \mathbf{div}\, \boldsymbol{\sigma}(\boldsymbol{\varphi}) = \mathbf{0} & \text{in } \Omega, \\ \boldsymbol{\sigma}(\boldsymbol{\varphi}) = \mathbf{C}\, \boldsymbol{\varepsilon}(\boldsymbol{\varphi}) & \text{in } \Omega, \\ \boldsymbol{\varphi} = \mathbf{0} & \text{on } \Gamma_D, \\ \boldsymbol{\sigma}(\boldsymbol{\varphi})\boldsymbol{n} = \mathbf{0} & \text{on } \Gamma_N. \end{cases}$$

We show that Proposition 2.2 can be illustrated in the case when Ω is a triangle in which the edges represent Γ_D, Γ_N and Γ_C (or also a trapezoid, see the Remark 3.1 hereafter) and the displacement fields $\boldsymbol{u}$ and $\bar{\boldsymbol{u}}$ are linear.

We consider the triangle Ω of vertexes $A = (0, 0)$, $B = (1, 0)$ and $C = (x_c, y_c)$ with $y_c > 0$ and we set $\Gamma_D =]B, C[$, $\Gamma_N =]A, C[$, $\Gamma_C =]A, B[$. The body Ω lies on a rigid foundation, the half-space delimited by the straight line (A, B) as depicted in Figure 1. We suppose that the body Ω is governed by Hooke's law concerning homogeneous

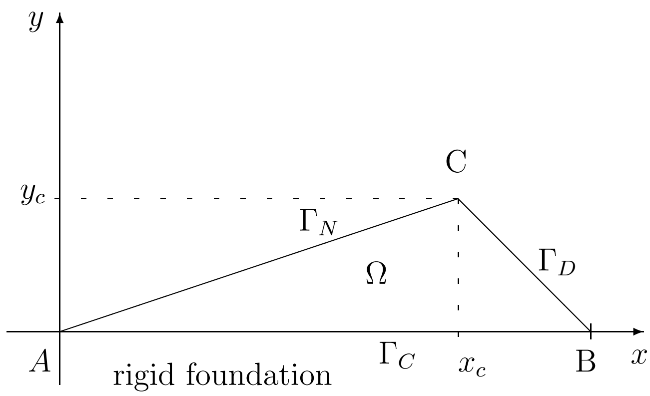

Figure 1: The geometry of the body Ω

isotropic materials so that (2.2) becomes

$$\boldsymbol{\sigma}(\boldsymbol{u}) = \frac{E\nu}{(1-2\nu)(1+\nu)} tr(\boldsymbol{\varepsilon}(\boldsymbol{u}))\mathbf{I} + \frac{E}{1+\nu}\boldsymbol{\varepsilon}(\boldsymbol{u}), \tag{3.2}$$

where $\mathbf{I}$ is the identity matrix, tr represents the trace operator, E and ν denote Young's modulus and Poisson's ratio, respectively with $E > 0$ and $0 \leq \nu < 1/2$. Let $(x = (1, 0), y = (0, 1))$ stand for the canonical basis of $\mathbb{R}^2$. We suppose that the volume forces $\boldsymbol{f} = (f_x, f_y) = (0, 0)$ are absent in Ω and that the surface forces on Γ_N are denoted by $\mathbf{F} = (F_x, F_y)$. Let $\mathbf{U} = (U_x, U_y)$ represent the given displacements on Γ_D.

We begin with the determination of $\boldsymbol{\varphi} = (\varphi_x, \varphi_y)$ in (3.1). The field $\boldsymbol{\varphi}$ is linear and $\varphi_y = 0$ on $\Gamma_C \cup \Gamma_D$ (since $u_y = \bar{u}_y = 0$ on Γ_C). Therefore we get $\varphi_y = 0$ in Ω. Moreover $\varphi_x = 0$ in Γ_D. Hence

$$\varphi_x = \alpha(y_c x + (1 - x_c)y - y_c), \tag{3.3}$$

$$\varphi_y = 0, \tag{3.4}$$

where $\alpha \in \mathbb{R} \setminus \{0\}$.

Inserting now the expressions (3.3)–(3.4) of $\boldsymbol{\varphi}$ in the constitutive law (3.2) gives

$$\boldsymbol{\sigma}(\boldsymbol{\varphi}) = \frac{\alpha E}{1+\nu} \begin{pmatrix} \dfrac{y_c(1-\nu)}{1-2\nu} & \dfrac{1-x_c}{2} \\ \dfrac{1-x_c}{2} & \dfrac{\nu\, y_c}{1-2\nu} \end{pmatrix}, \tag{3.5}$$

and $\mathbf{div}\,\boldsymbol{\sigma}(\boldsymbol{\varphi}) = \mathbf{0}$ in Ω. Then we consider the Neumann condition: $\boldsymbol{\sigma}(\boldsymbol{\varphi})\boldsymbol{n} = \mathbf{0}$ on Γ_N. Since the unit outward normal vector on Γ_N is $\boldsymbol{n} = (-y_c/\sqrt{x_c^2 + y_c^2}, x_c/\sqrt{x_c^2 + y_c^2})$, the stress vector on Γ_N becomes

$$\boldsymbol{\sigma}(\boldsymbol{\varphi})\boldsymbol{n} = \begin{pmatrix} \dfrac{\alpha E(2\nu y_c^2 - 2y_c^2 - x_c^2 + 2x_c^2\nu + x_c - 2x_c\nu)}{2(1-2\nu)(1+\nu)\sqrt{x_c^2 + y_c^2}} \\ \dfrac{\alpha E y_c(x_c - 1 + 2\nu)}{2(1-2\nu)(1+\nu)\sqrt{x_c^2 + y_c^2}} \end{pmatrix}.$$

Keeping in mind that $0 \le \nu < 1/2, y_c > 0, E > 0$ and $\alpha \ne 0$, the Neumann condition is equivalent to the two following equalities (3.6) and (3.7):

$$\nu = \frac{1 - x_c}{2}, \tag{3.6}$$

$$y_c = x_c\sqrt{\frac{1 - x_c}{1 + x_c}}. \tag{3.7}$$

Hence

$$x_c \in]0, 1[, \quad y_c = x_c\sqrt{\frac{1 - x_c}{1 + x_c}}. \tag{3.8}$$

The admissible line γ in which are located the pairs (x_c, y_c) satisfying (3.8) is depicted in Figure 2.

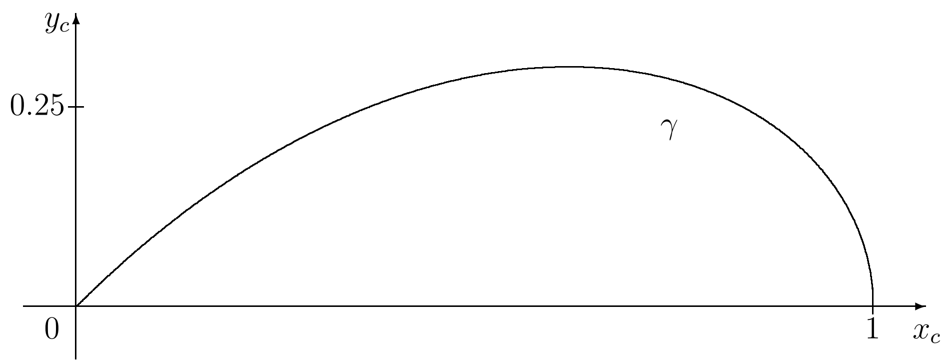

Figure 2: The admissible line γ for point $C = (x_c, y_c)$.

In this case the normal and tangential constraints on Γ_C given by (3.5) (with $\boldsymbol{n} = (0, -1)$, $\boldsymbol{t} = (1, 0)$, and denoting $\boldsymbol{\sigma_t}(\boldsymbol{\varphi}) = \sigma_t(\boldsymbol{\varphi})\boldsymbol{t}$) become

$$\sigma_n(\boldsymbol{\varphi}) = \frac{\alpha E(1 - x_c)}{3 - x_c}\sqrt{\frac{1 - x_c}{1 + x_c}}, \tag{3.9}$$

$$\sigma_t(\boldsymbol{\varphi}) = \frac{\alpha E(1 - x_c)}{x_c - 3}.$$

Remark 3.1 *If instead a triangle we consider a trapezoid of vertexes* $A = (0,0)$*,* $B = (\theta, 0)$*,* $C = (x_c, y_c)$ *and* $D = (x_c + \theta(1 - x_c), (1 - \theta)y_c)$ *with* $y_c > 0$ *and* $0 < \theta < 1$ *the discussion is the same as previously. In fact it suffices to define* $\Gamma_D =]C, D[$*,* $\Gamma_N =]A, C[\cup]B, D[$*,* $\Gamma_C =]A, B[$ *and to observe that the lines AC and BD are parallel (see Figure 3).*

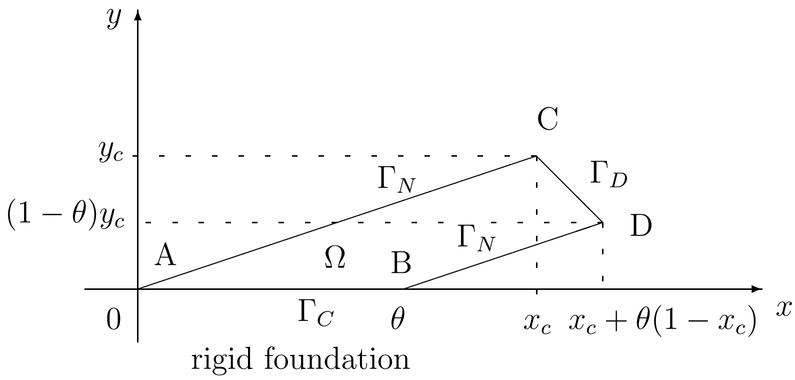

Figure 3: Case where Ω is a trapezoid

We now determine a the field $\boldsymbol{u} = (u_x, u_y)$ satisfying (2.1)–(2.6) and grazing contact. Since $\boldsymbol{u} = -\boldsymbol{\varphi}$ on Γ_C it can be written

$$\begin{aligned} u_x &= -\alpha y_c(x-1) + \delta y, \\ u_y &= \gamma y, \end{aligned}$$

with δ and γ in $\mathbb{R}$. Since $\alpha \neq 0$ we see that $\boldsymbol{u} \not\equiv \boldsymbol{0}$ on Γ_C and $\mathbf{div}\, \boldsymbol{\sigma}(\boldsymbol{u}) = \boldsymbol{0}$ in Ω. Inserting this expression in the constitutive law (3.2) and according to (3.6) and (3.7), we deduce that

$$\sigma_n(\boldsymbol{u}) = \frac{E}{3 - x_c} \left(\gamma \frac{1 + x_c}{x_c} - \alpha(1 - x_c) \sqrt{\frac{1 - x_c}{1 + x_c}} \right),$$

$$\sigma_t(\boldsymbol{u}) = \frac{\delta E}{x_c - 3},$$

on Γ_C. Since $\sigma_n(\boldsymbol{u}) = \sigma_t(\boldsymbol{u}) = 0$ (grazing contact), we deduce

$$\delta = 0, \qquad \gamma = \alpha x_c \left(\frac{1 - x_c}{1 + x_c} \right)^{\frac{3}{2}}.$$

The displacement field $\mathbf{U} = (U_x, U_y)$ incorporated in the Dirichlet condition on Γ_D becomes

$$U_x = -\alpha x_c \sqrt{\frac{1 - x_c}{1 + x_c}} (x - 1), \tag{3.10}$$

$$U_y = \alpha x_c \left(\frac{1 - x_c}{1 + x_c} \right)^{\frac{3}{2}} y. \tag{3.11}$$

The densities of surface forces $\boldsymbol{\sigma}(\boldsymbol{u})\boldsymbol{n} = \mathbf{F} = (F_x, F_y)$ on the boundary part Γ_N with $\boldsymbol{n} = (-\sqrt{(1-x_c)/2}, \sqrt{(1+x_c)/2})$ are then

$$F_x = \frac{2E\alpha x_c(1-x_c)\sqrt{2}}{(1+x_c)^{3/2}(3-x_c)}, \tag{3.12}$$

$$F_y = 0. \tag{3.13}$$

In the case where Ω is a trapezoid, it suffices to consider also the second part of Γ_N which is precisely the straight line segment BD depicted in Figure 3 with $\boldsymbol{n} = (\sqrt{(1-x_c)/2}, -\sqrt{(1+x_c)/2})$.

Having determined a field $\boldsymbol{u}$ which solves the friction problem (in fact (2.1)–(2.6) is satisfied for any $\mu \geq 0$), the next step consists of adding $\boldsymbol{u} + \boldsymbol{\varphi} = \bar{\boldsymbol{u}}$ and to check that the conditions of Proposition 2.2 are fulfilled. Clearly $\bar{\boldsymbol{u}}$ satisfies the equations in (2.7). Since $\sigma_n(\bar{\boldsymbol{u}}) = \sigma_n(\boldsymbol{u}) + \sigma_n(\boldsymbol{\varphi}) = \sigma_n(\boldsymbol{\varphi})$ on Γ_C and according to (3.9) we need

$$\alpha < 0.$$

Moreover the condition $|\sigma_t(\bar{\boldsymbol{u}})| \leq -\mu\sigma_n(\bar{\boldsymbol{u}})$ on Γ_C reduces to

$$\mu \geq \sqrt{\frac{1+x_c}{1-x_c}}.$$

We finally remark that the displacement field $\boldsymbol{u}$ moves points A, B and C to the new positions given by $\overline{A}$, $\overline{B}$ and $\overline{C}$ respectively.

$$\overline{A} = \left(\alpha x_c\sqrt{\frac{1-x_c}{1+x_c}}, 0\right),$$

$$\overline{B} = B = (1, 0),$$

$$\overline{C} = \left(x_c\left(1+\alpha\sqrt{\frac{1-x_c}{1+x_c}}(1-x_c)\right), x_c\sqrt{\frac{1-x_c}{1+x_c}}\left(1+\alpha x_c\left(\frac{1-x_c}{1+x_c}\right)^{\frac{3}{2}}\right)\right).$$

The field $\bar{\boldsymbol{u}}$ does not change the positions of A and B whereas C moves to $\overline{C}$ after deformation.

Proposition 3.2 *Let be given the triangle Ω of vertexes $A = (0,0)$, $B = (1,0)$ and $C = (x_c, y_c)$ with $y_c > 0$. Set $\Gamma_D =]B, C[$, $\Gamma_N =]A, C[$, $\Gamma_C =]A, B[$ and let $E > 0$, $\alpha < 0$. Assume that the pair (x_c, y_c) satisfies:*

$$x_c \in]0,1[, \quad y_c = x_c\sqrt{\frac{1-x_c}{1+x_c}}.$$

Set

$$\nu = \frac{1-x_c}{2},$$

and $\boldsymbol{f} = \mathbf{0}$*. Let the densities of surface forces* $\mathbf{F} = (F_x, F_y)$ *on* Γ_N *be given by* (3.12)–(3.13) *and let* $\mathbf{U} = (U_x, U_y)$ *on* Γ_D *be as in* (3.10)–(3.11)*.*

For any $\mu \geq \sqrt{\frac{1+x_c}{1-x_c}}$ *there exist at least two solutions of the Coulomb frictional contact problem* (2.1)–(2.6)*. The first solution is given by the field* $\boldsymbol{u} = (u_x, u_y)$ *satisfying grazing contact with slip: its expression is in* (3.10)–(3.11) *for all* $(x, y) \in \Omega$*. The second solution corresponds to stick: it is* $\bar{\boldsymbol{u}} = (\bar{u}_x, \bar{u}_y)$ *such that:*

$$\bar{u}_x = \alpha(1 - x_c)y,$$

$$\bar{u}_y = \alpha x_c \left(\frac{1 - x_c}{1 + x_c}\right)^{\frac{3}{2}} y,$$

for all (x, y) *in* Ω*.*

The same result holds when considering the trapezoid as in Remark 3.1. Note that one could add an additional (and not restrictive) smallness assumption on $|\alpha|$ which is not linked to the equations (2.1)–(2.6) but rather to the small strain hypothesis.

3.2. *Case where u satisfies separation*

In fact the class of multiple solutions involving grazing contact we obtained in section 3.1 can be seen as a limiting case of the following result proved in [9] which we recall hereafter.

Proposition 3.3 *Let be given the triangle* Ω *of vertexes* $A = (0, 0)$, $B = (1, 0)$ *and* $C = (x_c, y_c)$ *with* $y_c > 0$*. Set* $\Gamma_D =]B, C[$, $\Gamma_N =]A, C[$, $\Gamma_C =]A, B[$ *and let* $E > 0$, $\beta > 0$*. Assume that the pair* (x_c, y_c) *satisfies:*

$$x_c \in]0, 1[, \quad \sqrt{\frac{1}{4} + x_c - x_c^2} - \frac{1}{2} < y_c < x_c \sqrt{\frac{1 - x_c}{1 + x_c}}. \tag{3.14}$$

Set

$$\nu = \frac{(y_c^2 - x_c + x_c^2)^2}{((x_c - 1)^2 + y_c^2)(x_c^2 + y_c^2)},$$

and $\boldsymbol{f} = \mathbf{0}$*. Let the densities of surface forces* $\mathbf{F} = (F_x, F_y)$ *on* Γ_N *be given by*

$$\mathbf{F} = \begin{pmatrix} \dfrac{-E\beta y_c (x_c^2 - 2x_c + y_c^2)(y_c^2 + (x_c - 1)^2)^2 (x_c^2 + y_c^2)^{3/2}}{(2(x_c^2 - x_c + y_c^2)^2 + y_c^2)(x_c^3 - x_c^2 + x_c y_c^2 + y_c^2)} \\ 0 \end{pmatrix}.$$

Set $\mathbf{U} = (U_x, U_y)$ *on* Γ_D *as follows:*

$$U_x = \beta y_c \left(\frac{(x_c^2 - 2x_c + y_c^2) y_c}{x_c^3 - x_c^2 + y_c^2 x_c + y_c^2} (x - 1) + y \right), \tag{3.15}$$

$$U_y = -\beta y_c \left((x - 1) + \left(\frac{(y_c^2 - x_c + x_c^2)^2 (x_c^2 - 2x_c + y_c^2)}{y_c (x_c^3 - x_c^2 + x_c y_c^2 + y_c^2)} \right) y \right). \tag{3.16}$$

Then for any $\mu \geq x_c/y_c$ *there exist at least two solutions of the Coulomb frictional contact problem* (2.1)–(2.6)*. The first solution corresponding to strict separation is given by the field* $\boldsymbol{u} = (u_x, u_y)$ *whose expression is in* (3.15)–(3.16) *for all* $(x, y) \in \Omega$*. The second solution satisfies stick: it is* $\bar{\boldsymbol{u}} = (\bar{u}_x, \bar{u}_y)$ *such that:*

$$\bar{u}_x = \frac{2\beta x_c y_c((x_c-1)^2 + y_c^2)}{x_c^3 - x_c^2 + x_c y_c^2 + y_c^2} y,$$

$$\bar{u}_y = \frac{-\beta((x_c-1)^2 + y_c^2)(y_c^2 + y_c - x_c + x_c^2)(y_c^2 - y_c - x_c + x_c^2)}{x_c^3 - x_c^2 + x_c y_c^2 + y_c^2} y.$$

Proof. See [9]. □

The same result holds when considering the trapezoid as in Remark 3.1. The admissible domain Σ in which are located the pairs (x_c, y_c) satisfying (3.14) is depicted in Figure 4.

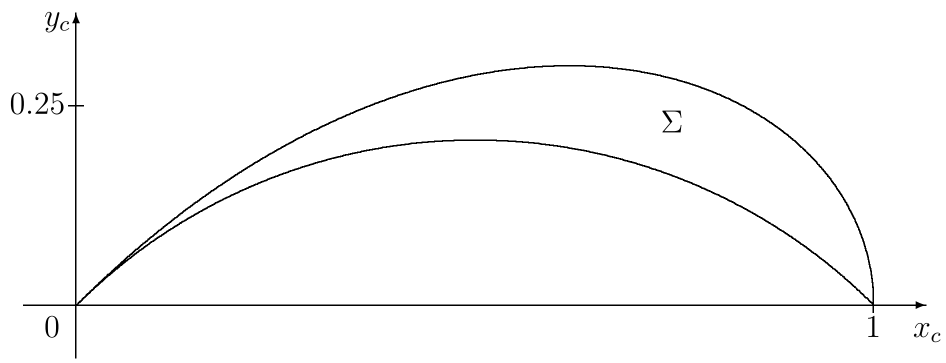

Figure 4: The open admissible region Σ for point $C = (x_c, y_c)$.

We remark that the displacement field $\boldsymbol{u}$ in Proposition 3.3 moves points A and C to the new positions

$$A' = \left(-\beta \frac{(x_c^2 - 2x_c + y_c^2) y_c^2}{x_c^3 - x_c^2 + y_c^2 x_c + y_c^2}, \beta y_c \right)$$

and

$$C' = \left(x_c + \beta \frac{2y_c^2 x_c((x_c-1)^2 + y_c^2)}{x_c^3 - x_c^2 + x_c y_c^2 + y_c^2}, \right.$$
$$\left. y_c - \beta \frac{y_c((x_c-1)^2 + y_c^2)(y_c^2 + y_c - x_c + x_c^2)(y_c^2 - y_c - x_c + x_c^2)}{x_c^3 - x_c^2 + x_c y_c^2 + y_c^2} \right), \quad (3.17)$$

respectively whereas position of point B remains unchanged. From the coordinates of A' we see that this field corresponds to a complete separation of Γ_C from the rigid foundation.

When considering the field $\bar{\boldsymbol{u}}$ in Proposition 3.3, the points A and B are stuck on the rigid foundation and point C admits after deformation the new coordinates given by C' in (3.17). This field corresponds to a sticking solution.

As in the previous study one could add an additional (and non restrictive) smallness assumption on β which is not linked to the equations (2.1)–(2.6) but rather to the small strain hypothesis.

Example 3.4 *We give an example satisfying the assumptions of Proposition 3.3 in which the geometry is a trapezoid (as in Remark 3.1) with* $\theta = 1/2$ *(hence* $B = (1/2, 0)$*). Set* $x_c = 3/4, y_c = 1/4$ *(so* (x_c, y_c) *satisfies* (3.14)*),* $\nu = 1/5, E = 1, \beta = 2/5$*. Set* $\boldsymbol{f} = \mathbf{0}$ *in* Ω*,* $\mathbf{F} = (F_x, F_y) = (-7\sqrt{10}/96, 0)$ *on* $]A, C[$*,* $\mathbf{F} = (F_x, F_y) = (7\sqrt{10}/96, 0)$ *on* $]B, D[$*,* $\mathbf{U} = (U_x, U_y) = (-3y/5, -3y/40)$ *on* $]C, D[$*. If the friction coefficient* μ *is such that* $\mu \geq 3$ *then both displacement fields* $\boldsymbol{u} = (u_x, u_y)$ *and* $\bar{\boldsymbol{u}} = (\bar{u}_x, \bar{u}_y)$ *defined by*

$$u_x = (7x + y - 7)/10, \quad u_y = (-4x - 7y + 4)/40,$$

and

$$\bar{u}_x = -3y/5, \quad \bar{u}_y = -3y/40,$$

are solutions of the Coulomb frictional contact problem (2.1)–(2.6)*. Figure 5 depicts the initial configuration* $\Omega = ABDC$ *(solid line) and the first deformed configuration corresponding to* $\boldsymbol{u}$*:* $\Omega' = A'B'D'C'$ *(dotted line). The second deformed configuration represents* $\bar{\boldsymbol{u}}$*: it is* $\Omega" = ABD'C'$ *(not depicted). Note that one could choose a smaller* β *to stay in the small strains range.*

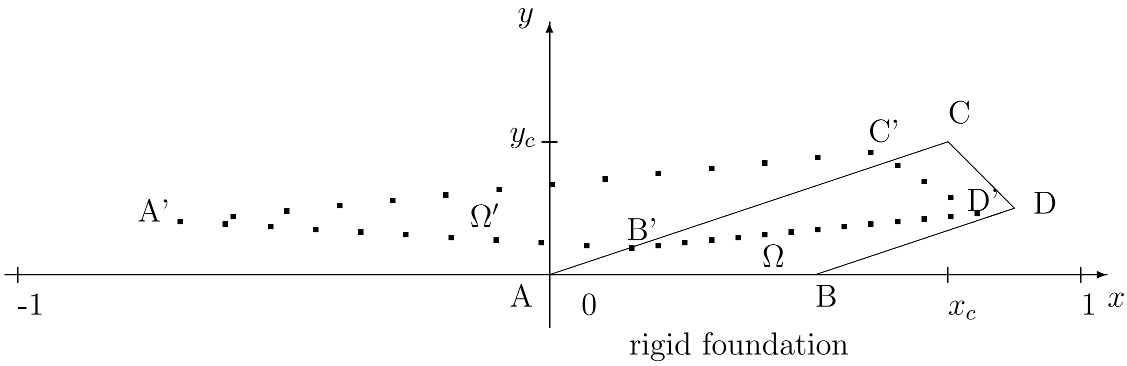

Figure 5: Initial configuration $\Omega = ABDC$ (solid line) and the first deformed configuration corresponding to separation $\Omega' = A'B'D'C'$ (dotted line). The second deformed configuration corresponding to stick is $\Omega" = ABD'C'$.

4. The finite element case

4.1. *The mixed finite element approximation*

The aim of this section is to translate in the finite dimensional case the discussion from the continuous context. In the forthcoming we use mixed finite elements with two multipliers representing the normal and the tangential constraints.

First of all, we have to introduce the mixed variational formulation for the continuous problems (2.1)–(2.6) and (2.7). Set

$$a(\boldsymbol{u},\boldsymbol{v}) = \int_\Omega (\mathbf{C}\boldsymbol{\varepsilon}(\boldsymbol{u})) : \boldsymbol{\varepsilon}(\boldsymbol{v})\, d\Omega, \qquad L(\boldsymbol{v}) = \int_\Omega \boldsymbol{f}\cdot\boldsymbol{v}\, d\Omega + \int_{\Gamma_N} \mathbf{F}\cdot\boldsymbol{v}\, d\Gamma,$$

for any $\boldsymbol{u}$ and $\boldsymbol{v}$ in the Sobolev space $(H^1(\Omega))^n$ (see [1]). In these definitions the notations $\cdot$ and $:$ represent the canonical inner products in $\mathbb{R}^n$ and $\mathcal{S}_n$ respectively. We define the sets of admissible displacement fields:

$$\mathbf{V} = \Big\{\boldsymbol{v} \in (H^1(\Omega))^n;\ \boldsymbol{v} = \mathbf{0} \text{ on } \Gamma_D\Big\}, \quad \mathbf{U}_{ad} = \Big\{\boldsymbol{v} \in (H^1(\Omega))^n;\ \boldsymbol{v} = \mathbf{U} \text{ on } \Gamma_D\Big\}.$$

The weak formulation of problem (2.1)–(2.6) is to find $(\boldsymbol{u},\lambda_n,\boldsymbol{\lambda_t}) \in \mathbf{U}_{ad}\times M_n \times \mathbf{M_t}(-\mu\lambda_n) = \mathbf{U}_{ad}\times\mathbf{M}(-\mu\lambda_n)$ verifying:

$$\left\{\begin{array}{ll} a(\boldsymbol{u},\boldsymbol{v}) - \displaystyle\int_{\Gamma_C} \lambda_n v_n\, d\Gamma - \int_{\Gamma_C} \boldsymbol{\lambda_t}\cdot\boldsymbol{v_t}\, d\Gamma = L(\boldsymbol{v}), & \forall \boldsymbol{v}\in\mathbf{V}, \\ \displaystyle\int_{\Gamma_C} (\nu_n - \lambda_n)u_n\, d\Gamma + \int_{\Gamma_C} (\boldsymbol{\nu_t} - \boldsymbol{\lambda_t})\cdot\boldsymbol{u_t}\, d\Gamma \geq 0, & \forall(\nu_n,\boldsymbol{\nu_t})\in\mathbf{M}(-\mu\lambda_n), \end{array}\right. \tag{4.1}$$

where $\mathbf{M}(-\mu\lambda_n) = M_n\times\mathbf{M_t}(-\mu\lambda_n)$ with $M_n = \{\nu\in H^{-\frac12}(\Gamma_C);\ \nu\leq 0 \text{ on } \Gamma_C\}$ and, for any $g\in -M_n$, $\mathbf{M_t}(g) = \{\boldsymbol{\nu}\in (H^{-\frac12}(\Gamma_C))^{n-1};\ |\boldsymbol{\nu}|\leq g \text{ on } \Gamma_C\}$. The notation $H^{-\frac12}(\Gamma_C)$ stands for the dual space of $H^{\frac12}(\Gamma_C)$ (see [1]) so that the inequality conditions incorporated in the definitions of M_n and $\mathbf{M_t}(g)$ must be understood in the dual sense. When $(\boldsymbol{u},\lambda_n,\boldsymbol{\lambda_t})$ solves (4.1), it is straightforward that $\lambda_n = \sigma_n(\boldsymbol{u})$ and $\boldsymbol{\lambda_t} = \boldsymbol{\sigma_t}(\boldsymbol{u})$.

We set

$$\mathbf{U}^0_{ad} = \Big\{\boldsymbol{v}\in\mathbf{U}_{ad};\ \boldsymbol{v} = \mathbf{0} \text{ on } \Gamma_C\Big\}.$$

The weak formulation of problem (2.7) is to find $(\bar{\boldsymbol{u}},\theta_n,\boldsymbol{\theta_t}) \in \mathbf{U}^0_{ad}\times H^{-\frac12}(\Gamma_C)\times (H^{-\frac12}(\Gamma_C))^{n-1}$ verifying:

$$a(\bar{\boldsymbol{u}},\boldsymbol{v}) - \int_{\Gamma_C} \theta_n v_n\, d\Gamma - \int_{\Gamma_C} \boldsymbol{\theta_t}\cdot\boldsymbol{v_t}\, d\Gamma = L(\boldsymbol{v}), \qquad \forall\boldsymbol{v}\in\mathbf{V}. \tag{4.2}$$

As above mentioned, we note that $\theta_n = \sigma_n(\bar{\boldsymbol{u}})$ and $\boldsymbol{\theta_t} = \boldsymbol{\sigma_t}(\bar{\boldsymbol{u}})$ when $(\bar{\boldsymbol{u}},\theta_n,\boldsymbol{\theta_t})$ stands for the unique solution of (4.2).

The body Ω is discretized by using a family of triangulations $(\mathcal{T}_h)_h$ made of finite elements of degree $k\geq 1$ where $h>0$ is the discretization parameter representing the greatest diameter of an element in $\mathcal{T}_h$. The set approximating $\mathbf{V}$ becomes:

$$\mathbf{V}_h = \Big\{\boldsymbol{v}_h\in(C(\overline{\Omega}))^n;\ \boldsymbol{v}_h|_T\in(P_k(T))^n\ \ \forall T\in\mathcal{T}_h,\ \boldsymbol{v}_h = \mathbf{0} \text{ on } \Gamma_D\Big\},$$

where $C(\overline{\Omega})$ stands for the space of continuous functions on $\overline{\Omega}$ and $P_k(T)$ represents the space of polynomial functions of degree $\leq k$ on T. We mention that any discussion concerning the convergence of the finite element problems towards the continuous models is out of the scope of this paper. Moreover we choose $k = 1$ in the forthcoming numerical experiments.

Let the notation $\mathbf{U}_h$ stand for a convenient approximation of $\mathbf{U}$ on Γ_D. We set

$$\mathbf{U}_{ad,h} = \Big\{ \boldsymbol{v}_h \in \mathbf{V}_h;\ \boldsymbol{v}_h = \mathbf{U}_h \text{ on } \Gamma_D \Big\}.$$

On the boundary of Ω, we keep the notation $\boldsymbol{v}_h = v_{hn}\boldsymbol{n} + \boldsymbol{v}_{ht}$ for any $\boldsymbol{v}_h \in \mathbf{V}_h$ and we denote by $(T_h)_h$ the family of $(n-1)$-dimensional meshes on Γ_C inherited by $(\mathcal{T}_h)_h$. Set

$$W_h = \Big\{ \nu = \boldsymbol{v}_h|_{\Gamma_C}.\boldsymbol{n};\ \boldsymbol{v}_h \in \mathbf{V}_h \Big\},$$

which is included in the space of continuous functions on Γ_C which are piecewise of degree k on $(T_h)_h$ and coincides with the latter space when $\overline{\Gamma}_C \cap \overline{\Gamma}_N = \emptyset$.

We denote by p the dimension of W_h and by $\psi_i, 1 \leq i \leq p$ the corresponding canonical finite element basis functions of degree k. For all $\nu \in W_h$ we shall denote by $F(\nu) = (F_i(\nu))_{1 \leq i \leq p}$ the generalized loads at the nodes of Γ_C:

$$F_i(\nu) = \int_{\Gamma_C} \nu \psi_i, \quad \forall\, 1 \leq i \leq p.$$

We define the sets of Lagrange multipliers: $M_{hn} = \{\nu \in W_h;\ F_i(\nu) \leq 0,\ \ \forall 1 \leq i \leq p\}$ and, for any $g \in -M_{hn}$, $\mathbf{M}_{ht}(g) = \{\boldsymbol{\nu} \in (W_h)^{n-1};\ |F_i(\boldsymbol{\nu})| \leq F_i(g),\quad \forall\, 1 \leq i \leq p\}$. Note that in the definition of $\mathbf{M}_{ht}(g)$ we make a slight abuse of notation when writing $F_i(\boldsymbol{\nu})$. This means in particular that $F_i(\boldsymbol{\nu})$ lies in $\mathbb{R}^{n-1}$.

Hence, the discrete problem issued from (4.1) becomes: *find* $(\boldsymbol{u}_h, \lambda_{hn}, \boldsymbol{\lambda}_{ht}) \in \mathbf{U}_{ad,h} \times M_{hn} \times \mathbf{M}_{ht}(-\mu\lambda_{hn}) = \mathbf{U}_{ad,h} \times \mathbf{M}_h(-\mu\lambda_{hn})$ *such that*

$$\left\{ \begin{array}{l} a(\boldsymbol{u}_h, \boldsymbol{v}_h) - \displaystyle\int_{\Gamma_C} \lambda_{hn} v_{hn}\, d\Gamma - \int_{\Gamma_C} \boldsymbol{\lambda}_{ht} \cdot \boldsymbol{v}_{ht}\, d\Gamma = L(\boldsymbol{v}_h), \qquad \forall \boldsymbol{v}_h \in \mathbf{V}_h, \\ \displaystyle\int_{\Gamma_C} (\nu_{hn} - \lambda_{hn}) u_{hn}\, d\Gamma + \int_{\Gamma_C} (\boldsymbol{\nu}_{ht} - \boldsymbol{\lambda}_{ht}) \cdot \boldsymbol{u}_{ht}\, d\Gamma \geq 0, \\ \qquad\qquad\qquad\qquad\qquad\qquad \forall (\nu_{hn}, \boldsymbol{\nu}_{ht}) \in \mathbf{M}_h(-\mu\lambda_{hn}). \end{array} \right. \tag{4.3}$$

We set

$$\mathbf{U}^0_{ad,h} = \Big\{ \boldsymbol{v}_h \in \mathbf{U}_{ad,h};\ \boldsymbol{v}_h = \mathbf{0} \text{ on } \Gamma_C \Big\}.$$

The discrete formulation of problem (4.2) is to find $(\bar{\boldsymbol{u}}_h, \theta_{hn}, \boldsymbol{\theta}_{ht}) \in \mathbf{U}^0_{ad,h} \times W_h \times (W_h)^{n-1}$ verifying:

$$a(\bar{\boldsymbol{u}}_h, \boldsymbol{v}_h) - \int_{\Gamma_C} \theta_{hn} v_{hn}\, d\Gamma - \int_{\Gamma_C} \boldsymbol{\theta}_{ht} \cdot \boldsymbol{v}_{ht}\, d\Gamma = L(\boldsymbol{v}_h), \qquad \forall \boldsymbol{v}_h \in \mathbf{V}_h. \tag{4.4}$$

It has been proven in [3], Proposition 3.2 that there exists at least a solution to Coulomb's discrete frictional contact problem (4.3) when $n = 2$. Besides it is straightforward that there is a unique solution to the problem (4.4). The following result is the discrete version of Proposition 2.2.

Proposition 4.1 *Let* $(\boldsymbol{u}_h, \lambda_{hn}, \boldsymbol{\lambda}_{ht})$ *be a solution of the problem* (4.3) *such that* $\boldsymbol{u}_h \not\equiv \mathbf{0}$ *on* Γ_C. *Let* $(\bar{\boldsymbol{u}}_h, \theta_{hn}, \boldsymbol{\theta}_{ht})$ *be the solution of problem* (4.4). *If* $\mu > 0$ *and* $|F_i(\boldsymbol{\theta}_{ht})| \leq -\mu F_i(\theta_{hn}), 1 \leq i \leq p$ *then* $(\bar{\boldsymbol{u}}_h, \theta_{hn}, \boldsymbol{\theta}_{ht})$ *is another solution of* (4.3).

Proof. Straightforward □

Remark 4.2 *The result in the proposition leads to two different solutions to the frictional contact problem, one of them corresponding to stick. Another problem considered in [7] consists of searching sufficient conditions leading to an infinity of slipping solutions, located on a continuous branch for precise (eigen)values of the friction coefficient.*

4.2. *Finite element computations*

This section is concerned with numerical experiments illustrating the previous discussions. There are four examples: the first three ones correspond to multiplicity with strict separation and stick and the last one deals with multiplicity involving grazing contact and stick.

In the first test we choose the trapezoidal geometry considered in Example 3.4 and we examine the convergence of the finite element method (4.3)–(4.4). We keep in mind that we have at our disposal in this case some solutions of the continuous problem (2.1)–(2.6). In the second experiment we keep the same geometry and we change the Poisson ratio and the loads in order to handle results where no solution to the continuous problem is available. In the third example we consider again a family of problems whose exact solutions are not known. We study the influence of the geometry and we exhibit numerical examples of non-uniqueness for small friction coefficients (such results are not available in the continuous case where the known non-uniqueness examples involve friction coefficients greater than 1). Finally in the fourth example we illustrate numerically Proposition 3.2.

As in section 3 we consider Hooke's constitutive law corresponding to homogeneous isotropic materials in (2.2):

$$\sigma_{ij}(\boldsymbol{u}) = \frac{E\nu}{(1-2\nu)(1+\nu)}\delta_{ij}\varepsilon_{kk}(\boldsymbol{u}) + \frac{E}{(1+\nu)}\varepsilon_{ij}(\boldsymbol{u}) \qquad \text{in } \Omega,$$

where $E > 0$ and $0 \leq \nu < 1/2$ stand for Young's modulus and Poisson's ratio, respectively. The implementation of problems (4.3) and (4.4) is achieved using the finite element code CAST3M developed at the Commissariat à l'Energie Atomique CEA - DEN/DM2S/SEMT.

4.2.1. *First example: case where* $\boldsymbol{u}$ *satisfies separation; numerical comparison with results of the continuous problem*

We consider the trapezoid $\Omega = ABDC$ introduced in Example 3.4. We recall the data: $A = (0,0), B = (1/2,0), C = (3/4,1/4), D = (7/8,1/8), \nu = 1/5, E = 1, \boldsymbol{f} = \mathbf{0}$ in Ω, $\mathbf{F} = (F_x, F_y) = (-7\sqrt{10}/96, 0)$ on $]A,C[$, $\mathbf{F} = (F_x, F_y) = (7\sqrt{10}/96, 0)$ on $]B,D[$, $\mathbf{U} = (U_x, U_y) = (-3y/5, -3y/40)$ on $]C,D[$.

An example of initial and deformed mesh is shown in Figure 6. Obviously one could choose some smaller **F** and **U** (the choice was made for a better graphical representation) to stay in the small strains range. We observe that the computed solution shows a complete separation of the body from the rigid foundation so that the solution does not depend on the friction coefficient (in fact the solution solves problem (4.3) for any $\mu \geq 0$).

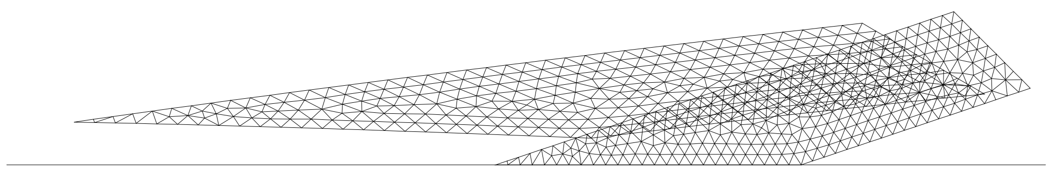

Figure 6: Initial and deformed mesh corresponding to $\boldsymbol{u}_h$ for problem (4.3)

Keeping the same mesh as in Figure 6, we solve the elasticity problem (4.4). In order to apply to result of Proposition 4.1 we need to check that $|F_i(\boldsymbol{\theta}_{h\boldsymbol{t}})| \leq -\mu F_i(\theta_{hn}), 1 \leq i \leq p$ (in this case $p = 26$). We observe that $F_i(\theta_{hn}) < 0$ for any $1 \leq i \leq 26$. Moreover $3 - 3.8\,10^{-13} \leq -|F_i(\boldsymbol{\theta}_{h\boldsymbol{t}})|/F_i(\theta_{hn}) \leq 3 + 2.6\,10^{-13}$, for any $1 \leq i \leq 26$. Consequently we deduce that $\boldsymbol{u}_h$ and $\bar{\boldsymbol{u}}_h$ solve problem (4.3) when $\mu \geq 3$. Note that this value is the "exact" one determined in Example 3.4. The initial mesh and both solutions (separation and stick) are shown in Figure 7.

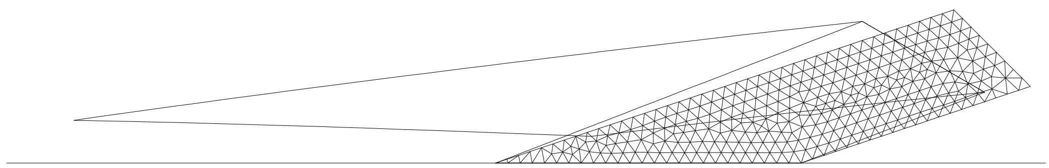

Figure 7: Initial mesh and both solutions $\boldsymbol{u}_h$ and $\bar{\boldsymbol{u}}_h$ for problem (4.3)

Next we determine the "minimal friction coefficient for multiplicity with separation and stick" defined by:

$$\max_{1 \leq i \leq p} -|F_i(\boldsymbol{\theta}_{h\boldsymbol{t}})|/F_i(\theta_{hn})$$

using different mesh sizes and we observe no variations of this minimal friction coefficient which ranges between 3 and $3 + 10^{-12}$. We end this example by noting that the computed stress fields are always uniform and the displacement fields are linear.

4.2.2. *Second example: influence of Poisson's ratio and of the loads*

We consider again the geometry of the first example and we perform the numerical experiments using 3-node triangles.

In the first discussion we keep the same data $\mathbf{F}, \boldsymbol{f}, \mathbf{U}$ as in the previous experiment and we change only Poisson's ratio. We compute the range of $-|F_i(\boldsymbol{\theta_{ht}})|/F_i(\theta_{hn})$ when $1 \leq i \leq p$ and we report the results in Table 1. When $\nu = 0$ and the mesh is coarse the solutions of (4.3) depend on the friction coefficient μ (this is not the case when $\nu = 0.1, 0.2, 0.3, 0.4, 0.45$ where the entire body separates from the rigid foundation). So we need to compute solutions using various friction coefficients and we observe numerically that the assumptions of Proposition 4.1 are never fulfilled. When $\nu = 0$ and the mesh is refined the solution separates strictly from the foundation but some forces $F_i(\theta_{hn})$ become positive. We observe that the displacement fields $\boldsymbol{u}_h$ and $\bar{\boldsymbol{u}}_h$ are not linear when $\nu \neq 0.2$. In particular the Von-Mises stress fields of $\boldsymbol{u}_h$ and $\bar{\boldsymbol{u}}_h$ increase near C (resp. D) if the Poisson's ratio is lower (resp. greater) than 0.2. Moreover the coefficient $\max_{1 \leq i \leq p} -|F_i(\boldsymbol{\theta_{ht}})|/F_i(\theta_{hn})$ seems to attain its minimum value when $\nu = 0.2$ (if p is large enough). We also remark that $\min_{1 \leq i \leq p} -|F_i(\boldsymbol{\theta_{ht}})|/F_i(\theta_{hn})$ attains its maximal value when $\nu = 0.2$.

Number of elements on Γ_C	1	10	100
$\nu = 0$	–	–	–
$\nu = 0.1$	[2.9228 , 2.9354]	[2.8650 , 3.5597]	[2.8766 , 13.254]
$\nu = 0.2$	[3.0000 , 3.0000]	[3.0000 , 3.0000]	[3.0000 , 3.0000]
$\nu = 0.3$	[3.0118 , 3.0689]	[2.5284 , 3.1406]	[1.0505 , 3.1194]
$\nu = 0.4$	[2.8357 , 3.1276]	[2.0666 , 3.3071]	[0.38794 , 3.2397]
$\nu = 0.45$	[2.4375 , 3.1484]	[1.7637 , 3.4310]	[1.7687 , 3.3033]

Table 1: Range of $-|F_i(\boldsymbol{\theta_{ht}})|/F_i(\theta_{hn}),\ 1 \leq i \leq p$

In the second discussion we modify the loads $\mathbf{F}$ and we keep the values of $\nu, \boldsymbol{f}$ and $\mathbf{U}$ as in the first example. We choose $p = 26$. When $\mathbf{F}$ is replaced with $\lambda\mathbf{F}$ the assumptions of the Proposition 4.1 remain true when $\lambda \in [0.77, 3.02]$. When λ decreases towards 0.77, a contact is established and we recover the phenomenon observed in the previous discussion with $\nu = 0$ and with coarse meshes. On the contrary if λ reaches 3.02 the solution $\boldsymbol{u}_h$ remains separated from the foundation but $\max_{1 \leq i \leq p} -|F_i(\boldsymbol{\theta_{ht}})|/F_i(\theta_{hn})$ tends to infinity. When $\lambda > 3.02$ some forces $F_i(\theta_{hn})$ become positive. Finally let us mention that if we replace simultaneously $\mathbf{F}$ and $\mathbf{U}$ by $\lambda\mathbf{F}$ and $\lambda\mathbf{U}$ with $\lambda > 0$ we have $-|F_i(\boldsymbol{\theta_{ht}})|/F_i(\theta_{hn}) = 3$ for any $1 \leq i \leq 26$.

4.2.3. *Third example: influence of the geometry*

We consider the parallelogram $\Omega = ABDC$ with $A = (0, 0)$, $B = (1, 0)$, $C = (1, H)$ and $D = (2, H)$, $(H > 0)$. The material characteristics are $E = 10000$ and $\nu = 0.25$.

The boundary $\Gamma_D =]C, D[$ is clamped: $\mathbf{U} = (0, 0)$ and no densities of body forces in Ω nor surface forces are applied on $]A, C[$. A load $\mathbf{F} = (-1, -4H/5)$ is applied on the remaining part $]B, D[$ of Γ_N. Therefore we obtain a family of problems depending on H. We observe numerically that for any choice of H (e.g., $H = 2, 5, 10, 50, 100$)

and for any choice of an uniform quadrangular mesh (e.g., with $5, 10, 20, 50$ elements on the contact zone) the computed solution of (4.3) shows a strict separation (and moves to the left). So it solves the friction problem for any $\mu \geq 0$.

The solution of problem (4.4) is computed and we observe that the assumptions of Proposition 4.1 are always fulfilled when the friction coefficient is large enough. The values of the minimal friction coefficient are reported in Table 2 (the symbol "..." means that the matrix sizes are too important for the computations). We first observe that for a given geometry the minimal friction coefficient converges well when the meshsize decreases. Moreover when H increases there are examples of non-uniqueness for small friction coefficients (lower than 0.5). From these examples which converge when the mesh size vanishes we can reasonably think that they become non-uniqueness examples for the continuous model (examples of non-unique solutions when $\mu \leq 1$ had not been obtained for the continuous model).

Number of elements on Γ_C	5	10	20	50
$H = 2$	1.6212	1.6261	1.6295	1.6307
$H = 5$	0.52609	0.52505	0.52371	0.52284
$H = 10$	0.39721	0.40068	0.40160	0.40196
$H = 20$	0.36031	0.37255	0.37814	0.38035
$H = 50$	0.33471	0.35319	0.36234	...
$H = 100$	0.32551	0.34624	...	...

Table 2: Value of $\max_{1\leq i\leq p} -|F_i(\boldsymbol{\theta}_{ht})|/F_i(\theta_{hn})$

4.2.4. *Fourth example: case where* $\boldsymbol{u}$ *satisfies grazing contact; numerical comparison with results of the continuous problem*

This example deals with solutions involving grazing contact (i.e., when $u_{hn} = \lambda_{hn} = 0$ on Γ_C) illustrating Propositions 3.2 and 4.1. So we consider the trapezoid $\Omega = ABDC$ with $A = (0, 0)$, $B = (1/2, 0)$, $C = (5/13, 10/39)$ $D = (9/13, 5/39)$. The material characteristics are $E = 10000$ and $\nu = 4/13$. The boundary $\Gamma_D =]C, D[$ is submitted to a prescribed displacement of $\mathbf{U} = (10(x - 1)/39, -40y/351)$, the boundaries $]B, D[$ (resp. $]A, C[$) are acted on by densities of surface forces: $\mathbf{F} = (-20E\sqrt{13}/459, 0)$ (resp. $\mathbf{F} = (20E\sqrt{13}/459, 0)$). No body forces are applied.

Figure 8 depicts an example of initial and deformed mesh. As previously we could choose some smaller $\mathbf{F}$ and $\mathbf{U}$ (the choice was made for a better graphical representation) to stay in the small strains range. We observe that the computed solution of (4.3) satisfies grazing contact. Consequently this solution solves problem (4.3) for any $\mu \geq 0$. Keeping the same mesh as in Figure 8, we solve the elasticity problem (4.4). In order to apply to result of Proposition 4.1 we need to check that $|F_i(\boldsymbol{\theta}_{ht})| \leq -\mu F_i(\theta_{hn}), 1 \leq i \leq 26$. We observe that $F_i(\theta_{hn}) < 0$ for any $1 \leq i \leq 26$ and $1.5 - 2.1\,10^{-14} \leq -|F_i(\boldsymbol{\theta}_{ht})|/F_i(\theta_{hn}) \leq 1.5 + 7\,10^{-14}$, for any $1 \leq i \leq 26$. Consequently we deduce that $\boldsymbol{u}_h$ and $\bar{\boldsymbol{u}}_h$ solve problem (4.3) when $\mu \geq 1.5$. Note that this value is the "exact" one according to Proposition 3.2. The initial mesh and both solutions (grazing contact and stick) are shown in Figure 9. We end this example by noting that for any mesh size we obtain the value 1.5 and that the displacement fields are linear.

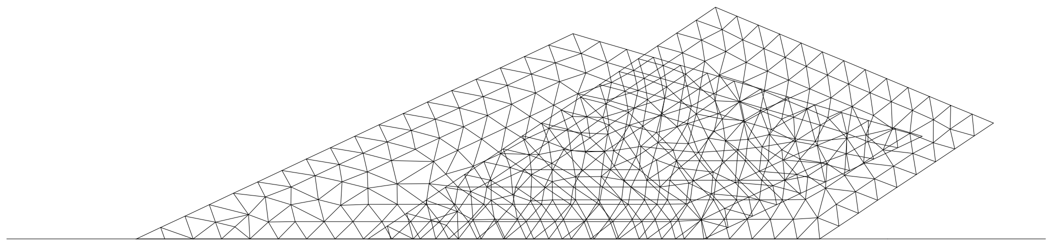

Figure 8: Initial and deformed mesh corresponding to $\boldsymbol{u}_h$ for problem (4.3)

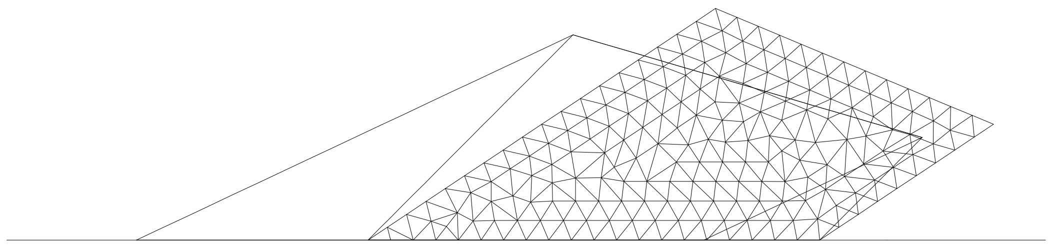

Figure 9: Initial mesh and both solutions $\boldsymbol{u}_h$ and $\bar{\boldsymbol{u}}_h$ for problem (4.3)

5. Concluding remarks

This paper considers a particular phenomenon (dealing with isolated stick solutions and solution multiplicity in the Coulomb friction problem) in the continuum and finite element contexts. We prove that the phenomenon occurs in the continuous case where two solutions with grazing contact and stick may solve the friction problem. Besides, from the good convergence of the computations (see example 3) we can reasonably deduce that such multiple solutions exist for the continuous model in the case of small friction coefficients.

Of course this work is a only a partial step in the complete classification process of all the pathologies in the unilateral contact model with Coulomb friction which is widely used in the engineering area. After a more complete understanding of the Coulomb friction model the main aim of these studies would be to furnish to the finite element code user a complete set of solutions at each time step and maybe also to propose a physically relevant solution among them, keeping in mind that the latter discussion is also non trivial.

Acknowledgments: The author is thankful to the referee for the remarks and suggestions which have led to several significant improvements in this paper.

References

[1] R. A. Adams, Sobolev Spaces (Academic Press, New-York, 1975).

[2] L.-E. Andersson, Existence results for quasistatic contact problems with Coulomb friction, *Appl. Math. Optim.*, 42 (2000) 169–202.

[3] P. Coorevits, P. Hild and M. Hjiaj, A posteriori error control of finite element approximations for Coulomb's frictional contact, *SIAM J. Sci. Comput.*, 23 (2001) 976–999.

[4] G. Duvaut and J.L. Lions, Les inéquations en mécanique et en physique (Dunod, Paris, 1972).

[5] C. Eck and J. Jarušek, Existence results for the static contact problem with Coulomb friction, *Math. Models Methods Appl. Sci.*, 8 (1998) 445–468.

[6] G. Fichera, Problemi elastostatici con vincoli unilaterali: il problema di Signorini con ambigue condizioni al contorno, *Atti Accad. Naz. Lincei Mem. Cl. Sci. Fis. Mat. Natur. Sez. I*, (8) 7 (1963/1964) 91-140.

[7] R. Hassani, P. Hild, I. Ionescu and N.-D. Sakki, A mixed finite element method and solution multiplicity for Coulomb frictional contact, *Comput. Methods Appl. Mech. Engrg.*, 192 (2003) 4517–4531.

[8] P. Hild, Non-unique slipping in the Coulomb friction model in two-dimensional linear elasticity, *Q. J. Mech. Appl. Math.*, 57 (2004) 225–235.

[9] P. Hild, Multiple solutions of stick and separation type in the Signorini model with Coulomb friction, *Z. Angew. Math. Mech.*, 85 (2005) 673–680.

[10] J. Jarušek, Contact problems with bounded friction. Coercive case, *Czechoslovak. Math. J.*, 33 (1983) 237–261.

[11] N. Kikuchi and J.T. Oden, Contact problems in elasticity: a study of variational inequalities and finite element methods (SIAM, Philadelphia, 1988).

[12] J. Nečas, J. Jarušek and J. Haslinger, On the solution of the variational inequality to the Signorini problem with small friction, *Boll. Unione Mat. Ital.*, 17-B(5) (1980) 796–811.

[13] R. Rocca and M. Cocu, Existence and approximation of a solution to quasistatic Signorini problem with local friction, *Int. J. Engrg. Sci.*, 39 (2001) 1233–1255.

[14] Y. Renard, A uniqueness criterion for the Signorini problem with Coulomb friction, preprint available at http://www-gmm.insa-toulouse.fr/.